

CONF

CONF-800942--27

**MASTER**

THE CURRENT STATUS OF METHODS FOR SHIELDING ANALYSIS\*

W. W. Engle

By acceptance of this article the publisher or recipient acknowledges the U.S. Government's right to retain a nonexclusive, irrevocable, and exclusive right in and to the copyright covering this article.

\*Research sponsored by the Reactor Research and Technology Division, U.S. Department of Energy under contract W-7405-eng-26 with the Union Carbide Corporation.

DISCLAIMER



20 2/77

1/77

# THE CURRENT STATUS OF METHODS FOR SHIELDING ANALYSIS

W. W. Engle

Oak Ridge National Laboratory  
Oak Ridge, Tennessee 37830, U.S.A.

## ABSTRACT

Current methods used in shielding analysis and recent improvements in those methods are discussed. The status of methods development is discussed based on needs cited at the 1977 International Conference on Reactor Shielding. Additional areas where methods development is needed are discussed.

## INTRODUCTION

This paper will focus on the shielding methods routinely used at the Oak Ridge National Laboratory and on the improvements made in those methods since the Fifth International Conference on Reactor Shielding, April 1977. There has been no direct funding for a large methods development program in transport methods and as a result no major new codes have appeared; however, there has been significant progress in improving calculational techniques in existing codes. These improvements will be discussed and compared with Nynatt's list of needed developments presented at the Fifth International Conference. Finally, one important area where development is needed will be mentioned briefly.

## DISCRETE ORDINATES METHODS

It is clear that the discrete ordinates method is the work horse of the shielding methods at ORNL. In a recent unpublished study to prepare benchmark calculations for a large computer acquisition at ORNL, it was determined that the DOT code used more time on the ORNL computing system than any other single program. The ancestry of the DOT codes is shown in Fig. 1. TIC and DDK were written in the FLOCO symbolic assembly language for the IBM 704-709-7090 machines. TIC was limited to R-Z geometry while DDK was the first two-dimensional code to allow a choice of X-Y, R-Z, or R- $\theta$  geometry. DDK allowed a mesh size of approximately 1200 intervals with isotropic scattering on an IBM 7090. With  $P_1$  scattering, the maximum number of intervals was reduced to about 800. DDF and 2DF were the first widely distributed two-dimensional codes written in the FORTRAN language. DOT was originally developed for the IBM 7090 and later adapted to run on the IBM 360 and CDC 6600 machines. Problem size was determined by the amount of memory available on the particular machine. All codes in the DOT series allowed an arbitrary expansion of the scattering cross sections and the DOT IV series also allows variable mesh and quadrature. DOT IV also determines the maximum number of rows of mesh related information which can be stored in core in order to solve a given problem in available memory. DOT 4.2 was transferred to the Radiation Shielding Information Center for distribution in February 1979.

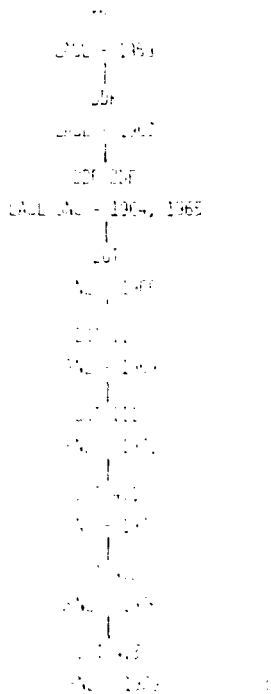


Fig. 1. Ancestry of the DOT Codes.

DOT 4.3 is the latest in the DOT series and offers diffusion acceleration of the inner iterations as well as the choice of the standard space dependent rebalance technique. Either method may be calculated on the fine mesh or a user defined coarse mesh. Although DOT 4.3 is awaiting complete testing and documentation before it is released for distribution, it is the only version maintained in-house at ORNL. Figure 2 shows a small portion of the iteration record for a large LMFBR shielding problem. In particular the convergence pattern of one energy group, as indicated by the "key flux," is highlighted. The key flux is the flux at a user selected mesh interval displayed for each iteration. Originally included for debugging purposes, the key flux has proven useful for convergence monitoring in a specific region of the problem and gives the user a "good feel" for the convergence in that region. The popularity of the key flux has prompted the suggestion that an array - approximately ten - of key flux locations be monitored to provide a more complete record of flux convergence.

The large problem capability of DOT IV is illustrated in Fig. 3 which shows a large loop design LMFBR geometry and isoflux contours calculated by DOT IV. The dimensions are large, approximately 8m x 24m, and require more than 30,000 mesh intervals. The calculation used  $P_1$  scattering cross sections. In terms of flux moment storage, this problem is more than 125 times larger than the maximum problem which could be run on DDK on existing computers in 1964. The area void of flux contours at the left center of the geometry contains the core, blanket and surrounding regions which were calculated in a separate DOT IV run. That calculation provided top, bottom and right boundary flux conditions used as sources for the larger calculation. Consistent multiple boundary sources are another feature of the DOT IV code.

SL	REBL	ERR*MAX	REBL*GRP	REBL*VOLM	ERR*KEY	FLUX*	NEG	FIX*	SOURCE
32	8.82E-03	7.00E+00	1.19E+00	1.00E+00	2.28E-02	0.0			2.49E+08
34	5.76E-03	1.26E+00	1.32E-02	4.95E-02	4.83E-02	0.0			2.49E+08
44	1.80E-05	5.90E-01	2.29E-03	1.91E-02	9.40E-02	0.0			2.49E+08
40	1.25E-05	2.40E-01	5.07E-04	1.22E-04	1.30E-01	0.0			2.49E+08
48	1.66E-05	5.84E-02	1.02E-04	2.23E-03	1.43E-01	0.0			2.49E+08
36	3.44E-05	1.93E-02	3.17E-05	9.60E-04	1.44E-01	0.0			2.49E+08
28	4.79E-05	1.09E-02	3.86E-05	2.74E-04	1.43E-01	0.0			2.49E+08
24	9.56E-05	6.67E-03	1.72E-05	8.43E-05	1.42E-01	0.0			2.49E+08
14	8.97E-05	3.32E-03	6.65E-06	3.85E-05	1.41E-01	0.0			2.49E+08
4	7.45E-05	7.73E-04	5.36E-06	2.01E-05	1.41E-01	0.0			2.49E+08
4	7.44E-05	3.92E-04	5.98E-07	7.87E-06	1.41E-01	0.0			2.49E+08
SL	REBL	ERR*MAX	REBL*GRP	REBL*VOLM	ERR*KEY	FLUX*	NEG	FIX*	SOURCE
72	4.55E-05	4.24E+00	1.19E+00	1.00E+00	4.01E-02	0.0			5.32E+08
58	3.50E-05	1.13E+00	1.67E-02	3.99E-02	7.55E-02	0.0			5.32E+08
52	4.60E-05	4.76E-01	1.93E-03	1.63E-02	1.41E-01	0.0			5.32E+08
38	5.66E-05	2.50E-01	1.04E-03	5.14E-04	2.01E-01	0.0			5.32E+08
44	4.73E-05	7.81E-02	2.21E-04	2.23E-03	2.29E-01	0.0			5.32E+08
36	7.31E-05	1.67E-02	7.85E-05	1.80E-03	2.35E-01	0.0			5.32E+08
40	4.75E-05	3.03E-03	4.71E-05	2.87E-04	2.34E-01	0.0			5.32E+08
24	8.41E-05	3.32E-03	2.31E-05	8.30E-05	2.32E-01	0.0			5.32E+08
14	7.17E-05	2.81E-03	9.66E-06	3.31E-05	2.31E-01	0.0			5.32E+08
4	7.42E-05	7.19E-04	2.44E-06	1.50E-05	2.31E-01	0.0			5.32E+08
4	8.09E-05	2.84E-04	2.92E-06	3.49E-06	2.31E-01	0.0			5.32E+08
SL	REBL	ERR*MAX	REBL*GRP	REBL*VOLM	ERR*KEY	FLUX*	NEG	FIX*	SOURCE
54	4.88E-05	3.23E+00	1.19E+00	1.00E+00	7.91E-02	0.0			9.28E+08
48	4.86E-05	7.77E-01	1.56E-02	2.96E-02	1.26E-01	0.0			9.28E+08
42	4.47E-05	2.53E-01	1.45E-03	1.22E-02	1.78E-01	0.0			9.28E+08
54	4.71E-05	1.59E-01	1.08E-03	9.79E-04	2.27E-01	0.0			9.28E+08
46	5.15E-05	7.03E-02	3.72E-04	1.96E-03	2.54E-01	0.0			9.28E+08
38	7.97E-05	2.12E-02	1.41E-04	8.42E-04	2.64E-01	0.0			9.28E+08
54	8.36E-05	5.59E-03	5.66E-05	2.37E-04	2.66E-01	0.0			9.28E+08
6	7.31E-05	1.94E-03	2.29E-05	6.36E-05	2.65E-01	0.0			9.28E+08
6	7.28E-05	1.61E-03	7.21E-06	2.37E-05	2.65E-01	0.0			9.28E+08
6	7.55E-05	9.40E-04	1.97E-06	9.67E-06	2.64E-01	0.0			9.28E+08

FIG. 2. Typical Convergence Pattern in DOT-IV Calculations.

The variable mesh (blocks of rows may have different mesh) and variable quadrature (quadrature varies by user defined zone) options in DOT IV are valuable options for special problems. Recent coding revisions in DOT 4.3 have reduced the cost penalty for the variable mesh option to approximately zero and use of that option is expected to increase.

The DOT codes have always offered the user a choice of flux extrapolation models and recent work by Tomlinson, et al. has provided users with the most definitive information thus far concerning appropriate flux models for a particular problem. Some of the conclusions of that work are:

1. In source-geometry combinations typical of many shielding problems, different flux extrapolation models do not converge to a single solution as the space mesh is refined.
2. In those same source-geometry combinations, the positive flux extrapolation models are required regardless of the degree to which the mesh is refined.
3. In typical shielding problems, the error due to finite mesh spacing may be greater than the variations between flux extrapolation models.

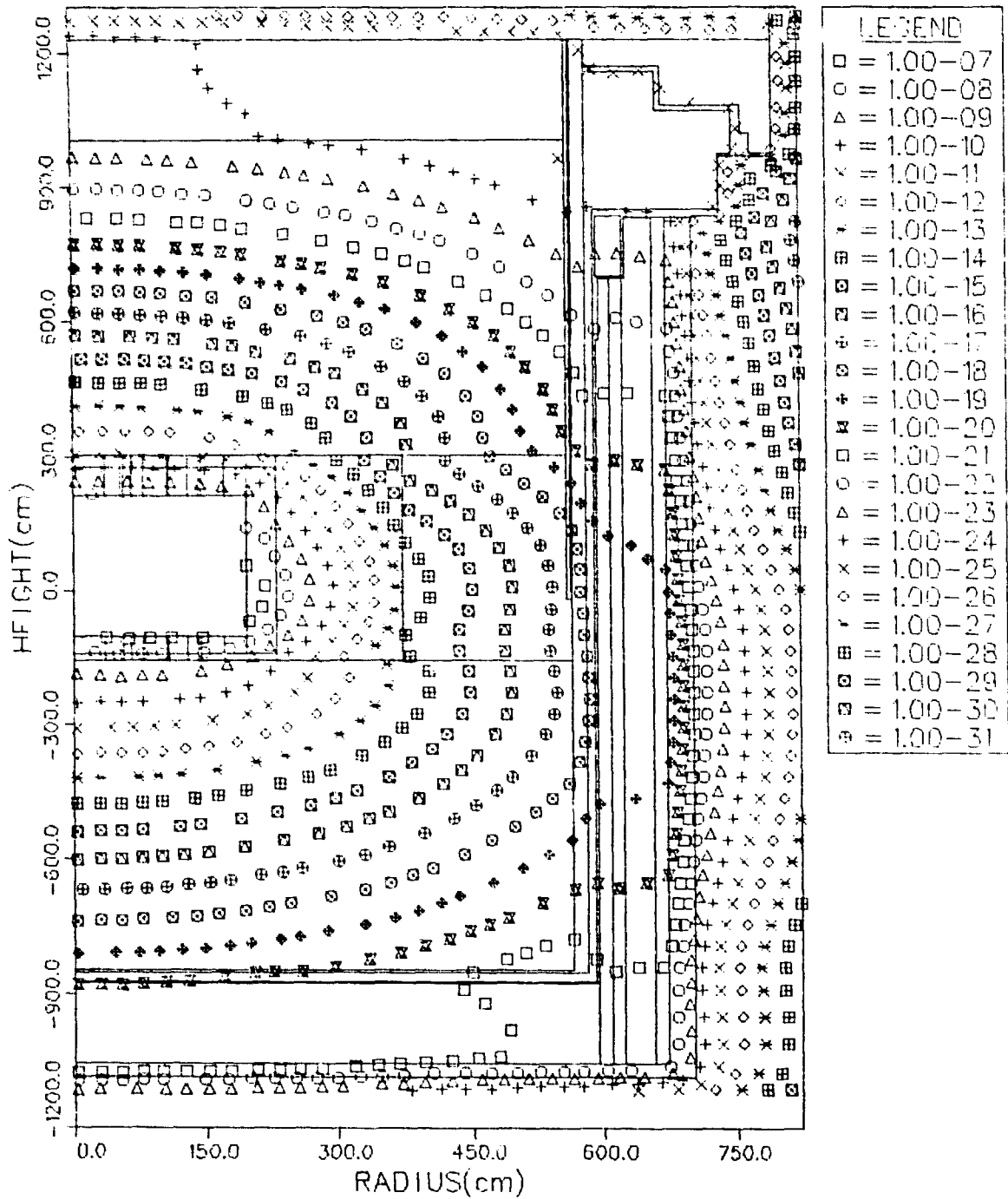


Fig. 3. An LMFR Loop Design Geometry with Flux Contours.

4. The theta-weighted model appears to most consistently avoid erratic behavior as mesh spacing is increased.
5. The linear (diamond) model with a consistent set-to-zero fixup model should probably be restricted to eigenvalue calculations.
6. The linear model with a step model fixup, long used in GRML codes, should be discarded.

This report also examined in detail the differences between TACTANK and IIT and as a result completely explained differences in the calculational results of the two codes.

#### SENSITIVITY AND CONTRIBUTION CALCULATIONS

Sensitivity and contribution calculations are now in routine use in both design analysis and experiment analysis. Two examples from the CCFR sup critical analysis program are presented. Figure 4 shows a DCF geometry for the CCFR downflow design with isoflux contours for neutrons with energy less than 2.38 eV. The concern in this calculation is the low energy flux at the DCF liner which peaks just above the wraparound shield near the lower right side of the figure. Figure 5 is a contribution plot for the lower portion of the geometry of Fig. 4. The response function used as a source in the adjoint calculation is the neutron flux less than 2.38 eV. The contribution plot clearly shows the large contribution through the streaming path between the outer radial shield and the wraparound shield. The plot also shows a significant contribution through the outer radial shield above the wrap-around shield and the thermalization in the concrete behind the liner which returns low energy neutrons to the liner.

Figure 6 shows the geometry, neutron flux and contribution flux for a calculation of the CCFR grid-plate shield experiment. A source of neutrons from the Tower Shielding Facility reactor enters the top of the R-Z geometry, streams through the 'L' shaped void region and produces fissions in the fuel rod array. The experiment measured the attenuation through the grid-plate shield which is the region just below the fuel rod array. This shield is a steel plate containing tapered holes. The neutron flux plot displays two prominent peaks, one in the concrete plug above the rod array and another due to fission neutrons produced in the fuel rod array. The contribution plot, which displays the spatial distribution of those neutrons which penetrate the grid-plate shield, shows that almost all of those neutrons are generated by fission in the lower portion of the fuel rod array. The lower portion of the contribution plot also clearly displays peaks corresponding to the holes in the grid-plate shield. The value of the contribution plot is shown rather dramatically in this figure; the important neutrons are not near the area where the peak neutron flux occurs which is typical of many shielding problems.

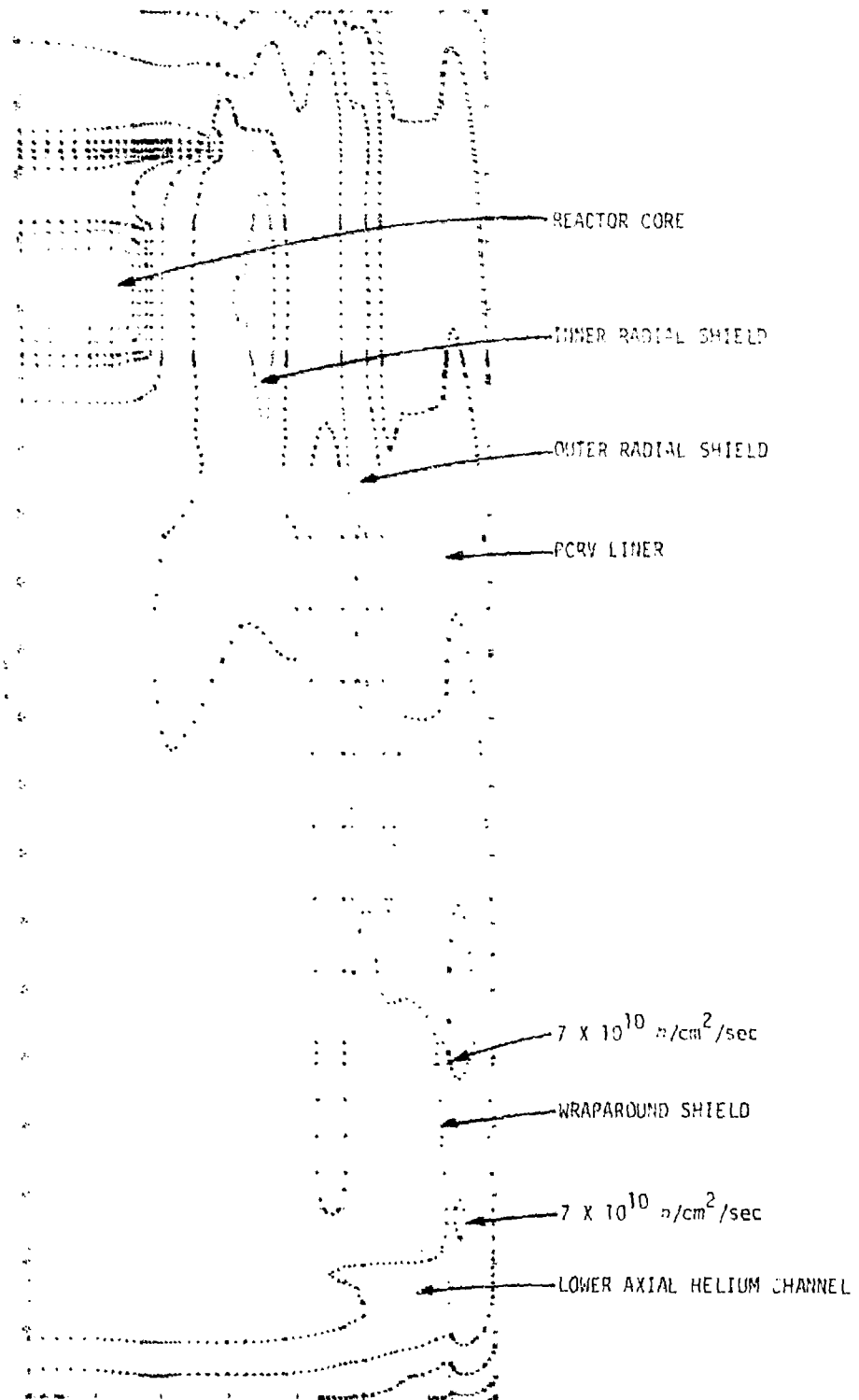


Fig. 4. A GCFR Downflow Design Geometry with Low Energy Flux Contours ( $E < 2.38 \text{ eV}$ ).

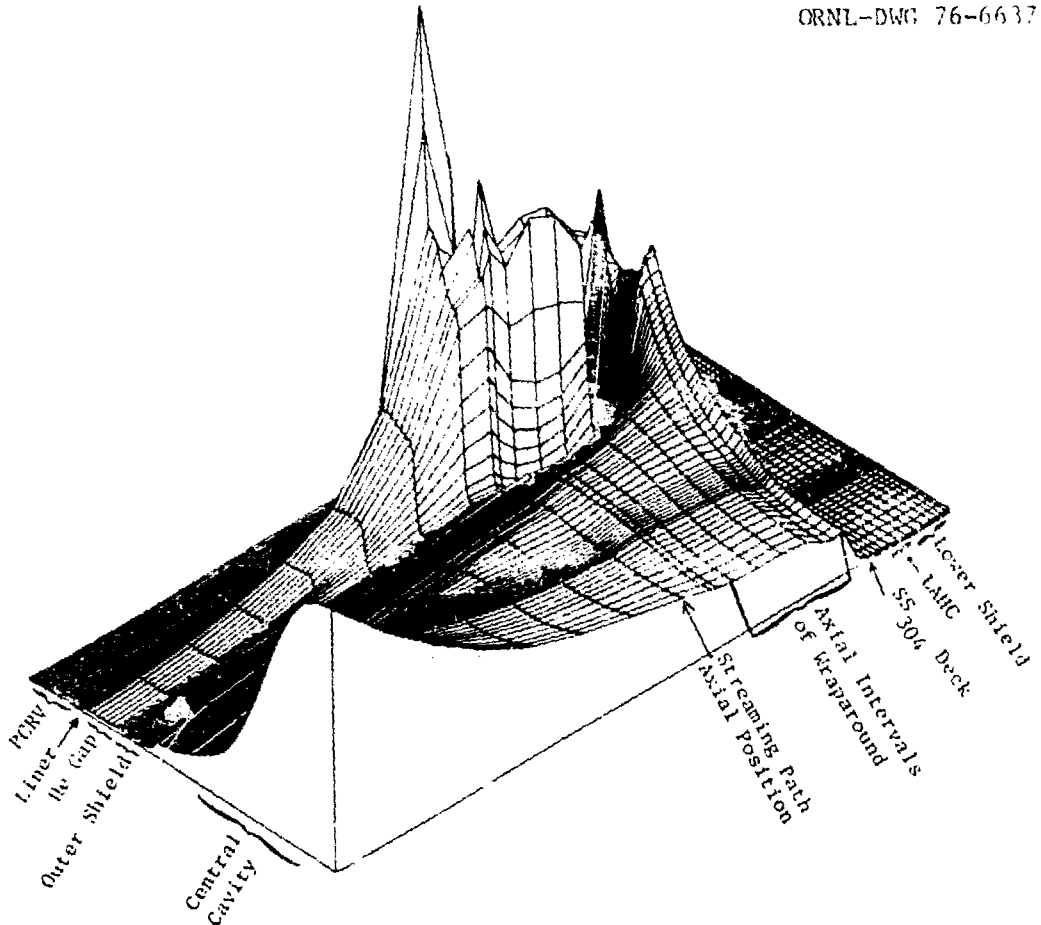


Fig. 5. Contribution Plot for GCFR Downflow Geometry.

#### DISCRETE ORDINATES COUPLING AND FORWARD-ADJOINT FOLDING

Coupled discrete ordinates calculations or bootstrap techniques and forward-adjoint folding were first extensively developed for analysis of the Fast Flux Test Facility. The method of forward-adjoint folding has been extended to off-axis cylinders. Figure 7 is a simple representation of an LIFBR design with an in-vessel decay heat removal heat exchanger (DRHX). DOT 4.3 was used to calculate the forward neutron fluxes which occur in the sodium pool without the presence of the DRHX. A DOT adjoint calculation was performed for the DRHX using the activation cross section for the secondary loop coolant as a source. The adjoint angle dependent flux at the outer boundary of the DRHX was then folded with a forward angle dependent flux regenerated from the flux moments in the large forward calculation. This technique allows the analyst to easily examine the effects of different heat exchanger designs and modifications to the heat exchanger shield configuration. The methods used to regenerate the forward angular flux in the quadrature and coordinate system of the adjoint DRHX calculation are very similar to the methods used to manipulate the quadrature and coordinate system in the coupling technique described in the following paragraph.



ORNL-DWG 77-14664

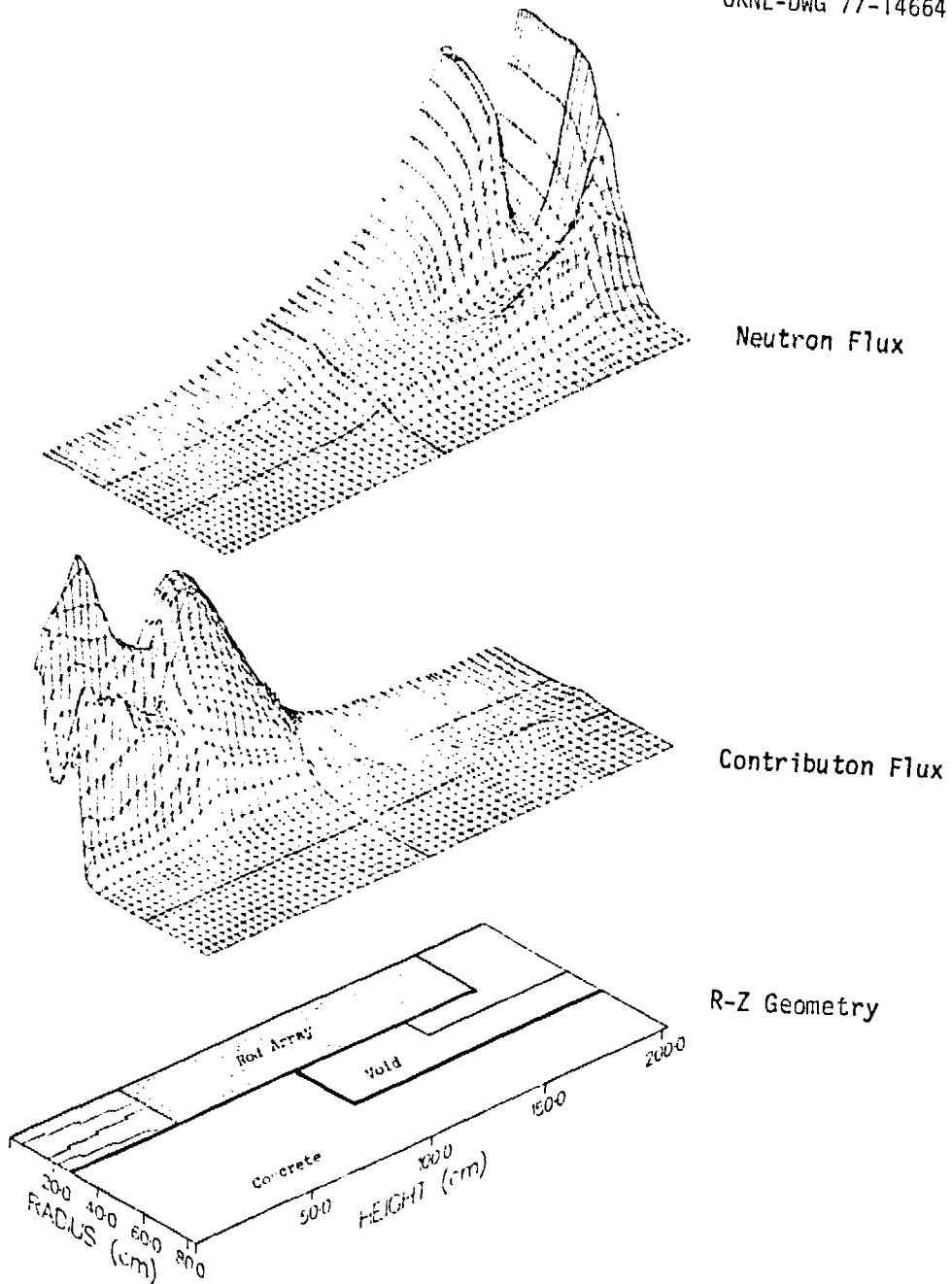


Fig. 6. Geometry, Contributor Flux, and Neutron Flux for the GCFR Grid-Plate Shield Experiment.

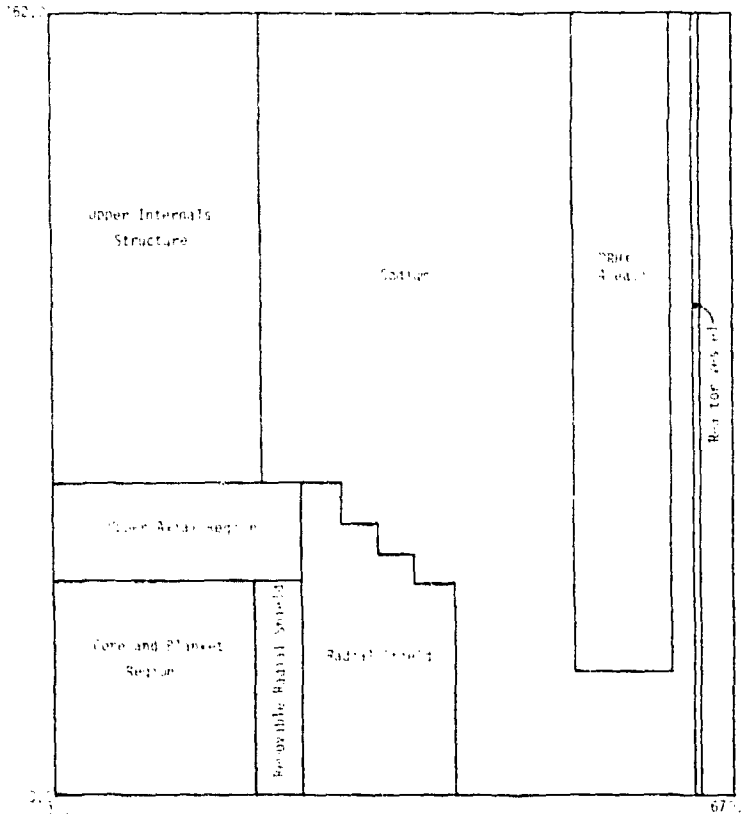


Fig. 7. Simplified Geometry Model for LMFBR Loop Design with In-Vessel Decay Heat Removal Heat Exchangers.

The method of coupling two discrete ordinates calculations using the angle dependent fluxes at a common boundary was extended recently to two cylinders which intersect at a  $90^\circ$  angle.<sup>6</sup> The preparation of an axial boundary source for the second cylinder involves the transformation of the quadrature from the coordinate system of the first cylinder to the coordinate system of the second cylinder and the mapping of the fluxes in the resulting quadrature into the desired quadrature for the second cylinder. This method was used to calculate a pipe chaseway experiment containing two  $90^\circ$  bends.<sup>7</sup> Figure 8 is a drawing of the experimental arrangement of the pipe chaseway experiment. The agreement between calculation and experiment on the exit centerline of pipe no. 4 was within a factor of two after nine orders of magnitude attenuation.

#### ALBEDO MONTE CARLO

The MORSE Monte Carlo code has been modified to apply a albedo boundary condition at specified surfaces within the geometry. This revised code was used to calculate the pipe chaseway experiment in Fig. 8 with much of the concrete wall represented as an albedo surface. The standard Monte Carlo technique with full transport in the concrete walls requires considerable computing time to follow the thermal neutrons in the concrete. The series of calculations in this study indicated that the protruding concrete corners

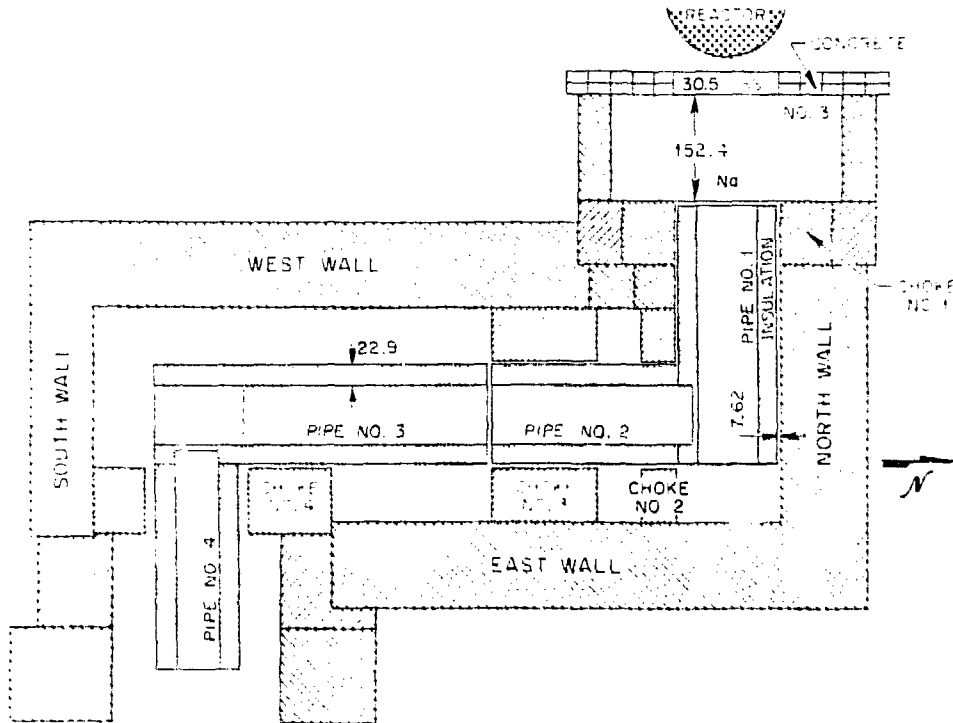


Fig. 8. Experimental Arrangement for Pipe Chaseway Containing Four Coolant Pipe Sections.

required a wedge-shaped region of full transport to account for those particles which penetrated the corner and emerged in the next leg of the chaseway. The agreement of the Monte Carlo calculation and the experiment along the centerline of the first two legs of the chaseway was within thirty percent. The third leg was not calculated.

#### STATUS UPDATE

In 1977 Mynatt<sup>1</sup> listed five areas where methods development was needed. These five areas are listed below with comments about the progress made in each area.

1. Improved Monte Carlo - discrete ordinates coupling, specifically volume coupling for use with adjoint difference techniques. Volume coupling has not been used extensively and there has been little work in this area. The increased capability for surface coupling mentioned previously for off-axis cylinders is also applicable to discrete ordinates - Monte Carlo coupling.
2. Improved Monte Carlo biasing methods that are easily understood by the user. The TRIPOLI<sup>8</sup> code provides improved biasing but the intricacies involved in using that biasing are very complex. Correlated tracking is an interesting development which is discussed in another paper in this meeting.<sup>9</sup>

3. Three-dimensional O-R-Z discrete ordinates code. Both LASL and Japan have three-dimensional X-Y-Z codes and LASL also has a Hex-Z code. The LASL codes were developed primarily for testing three-dimensional techniques and are limited to  $P_1$  scattering. The Japanese code is to be discussed in another paper in this meeting.<sup>10</sup> The O-R-Z geometry is still the most applicable geometry for large reactor shielding problems.
4. Improved semi-empirical techniques, especially for multilegged ducts. The albedo Monte Carlo discussed briefly is certainly less expensive but does not satisfy the semi-empirical definition.
5. Parametric verification experiments for streaming problems. There has been no additional work in this area.

In addition to the areas mentioned above, the advent of large vector processing machines such as the CRAY-1 and the recently announced Control Data Corporation Cyber 205 should prompt the development of new solution algorithms for the discrete ordinates method which take advantage of the vector capabilities of these machines. This work could lead to dramatic reductions in CPU time and pave the way for the much needed O-R-Z three-dimensional discrete ordinates code.

#### REFERENCES

1. F. R. MYNATT, "Shielding Methods Development in the United States," in Proc. of the Fifth International Conference on Reactor Shielding (1977).
2. W. A. RHOADES et al, "The DOT-IV Two-Dimensional Discrete Ordinates Transport Code with Space Dependent Mesh and Quadrature," ORNL/TM-6529 (January 1979).
3. E. T. TOMLINSON et al, "Flux Extrapolation Models Used in the DOT IV Discrete Ordinates Neutron Transport Code," ORNL/TM-7033 (May 1980).
4. K. D. LATHROP and F. W. BRINKLEY, "TWOTRAN-II: An Interfaced, Exportable Version of the TWOTRAN Code for Two-Dimensional Transport," LA-4848-MS (July 1973).
5. L. S. ABBOTT and F. R. MYNATT, "Review of the ORNL Radiation Shielding Analyses of the Fast Flux Test Facility Reactor," ORNL-5027 (July 1975).
6. M. L. WILLIAMS and W. W. ENGLE, JR., "Analysis of Streaming Through the Primary Coolant Pipe Chaseway of the Clinch River Breeder Reactor," Trans. Am. Nucl. Soc., 27, 779 (1977).
7. R. E. MAERKER, "Discrete Ordinate Analysis of the TSF Experiment on Neutron Streaming in a CRBR Prototypic Coolant Pipe Chaseway," ORNL/TM-6497 (November 1978).